JOURNAL of QASSIM UNIVERSITY FOR SCIENCE
Vol. 1, Issue 1, pp 64-79 (October 2022)
JQUS

Structural, Morphological and Optical Properties of Thermally Evaporated ZnS Thin Films

Fatimah G. Albadrani[a], Aicha Loucif[b*] and Saleh N. Alamri[c]

[a]*Department of physics, College of Science, Qassim University, P.O.95 Riyad Alkhabra, 51961, Saudi Arabia*
[b]*Department of physics, College of Science, Qassim University, P.O.64, Buraidah, 51452, Saudi Arabia*
[c]*Department of physics, Faculty of Sciences, Taibah University, P.O. Box 344, Medina, Saudi Arabia*

Corresponding author: f2013mb@hotmail.com

Abstract

The present study reports the effect of the substrate temperature on the structural, morphological, and optical properties of ZnS semiconducting thin films grown via thermal evaporation technique. These properties have been thoroughly investigated using X-ray diffraction (XRD), atomic force microscopy (AFM), and UV-visible spectroscopy. The deposition was performed on a glass substrate at room temperature (RT), 100, 150, and 250°C. Energy dispersive spectrometry (EDS) analysis revealed a high purity of the ZnS films and non-stoichiometry atomic ration of Zn:S. The synthesized films exhibited cubic structure and developed on the (111) preferential orientation plane. Furthermore, increasing the substrate temperature improved the crystallinity and surface morphology of the thin films. Compared to others deposited films, the film grown at 250°C exhibited relatively high transparency in visible light (~87%), high absorption of the ultra violet (UV) light (~94 %.), and wide band gap (3.80 eV). Moreover, the refractive index was evaluated using Herve–Vandamme, Reddy, and Kumar and Singh models, and then compared. In general, these findings revealed that ZnS thin films can be used as the buffer layer in copper indium gallium selenide (CIGS) based solar cells.

Keywords: *ZnS thin films, thermal evaporation, substrate temperature, optical properties*

1. Introduction

Zinc sulfide (ZnS) is an n-type semiconductor that belongs to the II-VI group and has wide band gap energy of 3.54 to 3.72 eV for cubic structures and 3.74 to 3.91 eV for hexagonal structures **[1].** Wide band gap, low-toxicity, low absorption in visible and infrared (IR) regions, high refractive index, and good transparency make ZnS highly desirable for diverse applications in various fields including light-emitting diodes (LEDs), nano-sensors, photocatalysis, lasers, flat panel displays, optometric applications, gas sensors, and solar cells **[2-4].**

ZnS thin films have been grown using different physical and chemical techniques such as ultrasonic spray technique **[1],** microwave-assisted chemical bath deposition method **[4],** electrochemical deposition **[5],** pulsed laser deposition **[6],** thermionic vacuum arc (TVA) **[7],** electron beam (e-beam) evaporation technique **[8],** successive ionic layer adsorption and reaction (SILAR) **[9],** and thermal evaporation technique **[10, 11].** Among several of physical techniques**, t**hermal evaporation is known to fabricate homogeneous films with good adhesion **[11].** The thermal evaporation technique entails evaporating the source material via a resistively heated boat under high vacuum conditions. Typically, the source material decomposes into constituent element vapour which will then traverse between the boat and the substrate. As a result, a high vacuum is required to augment the mean free path of the vapour particles. When the particles reach the substrate, they settle and are adsorbed into it to form a thin film.

Since the synthesis techniques as well as preparation conditions can influence the characteristics of ZnS films, this study deals with the effect of substrate temperature on the microstructural, morphological, and optical properties of the thermally evaporated ZnS thin films. In this respect, ZnS thin films were grown on glass substrate at room temperature (RT), 100, 150, and 250°C under high vacuum. The obtained results showed that varying the deposition temperature has a notable influence on inproving the physical properties of ZnS thin films, making them suitable for use as a buffer layer in copper indium gallium selenide (CIGS) based solar cells.

2. Experimental details

2.1 Thin Film preparation

Before deposition, the glass substrates were ultrasonically cleaned with liquid detergent (Decon 90) and distilled water for about one hour, respectively and then dried using N_2 gas. The films were deposited on well-cleaned substrates by using the thermal evaporation technique under vacuum of about 10^{-5} mba. High purity ZnS powder (99.999% from Sigma Aldrich) was used as source material.

First, 170 mg of ZnS powder was deposited within a molybdenum boat, and the substrate was placed in a holder and held 13.5 cm away from the evaporation source. To measure the temperature of the substrate, a thermocouple was maintained on the substrate holder. In order to achieve uniform film, the substrate holder was linked to an electric motor to rotate the substrate during the deposition. After that, the glass substrate was heated with a thermal heater to achieve the sample temperature required to begin the deposition process. Finally, the deposition process began as the boat was heated up by passing a high current of 110 A, causing the materials to evaporate and deposit on the substrate. The films were deposited on glass substrate for 45 min at room temperature (RT), 100, 150, and 250°C.

2.2 Characterization techniques

The thickness of the deposited thin films was estimated using surface scanning technique by Veeco DEKTAK 150 profilometer. An energy dispersive spectrometry (EDS) equipment connected to a desktop scanning electron microscope was used to analyze the constituent elements of the films (JCM-6000). X-ray diffraction (XRD) analysis were carried out to study the crystallographic properties of thin films using a (shimadzu D6000 XRD) device with a CuKα (**λ** = 0,15406 nm) radiation source. The surface morphology of the thin films was investigated through an atomic force microscopy (AFM) of the type (veeco di CP-II). The optical properties of the films were investigated using a Shimadzu UV-3101 PC spectrophotometer in the UV–VIS wavelength range of 200-800 nm.

3. Results and discussion

3.1 EDX analysis

EDX analysis was used to determine the elemental composition of the prepared films. The obtained spectra are shown in **Fig.1**. As can be seen, the presence of Zn and S demonstrates that the ZnS phase was successfully formed without any impurities, thus indicating the high purity of the films. However, the prepared ZnS films were non-stoichiometric Zn and S (**Table 1**) due to a difference between vapour pressure of Zn and S atoms **[12]**.

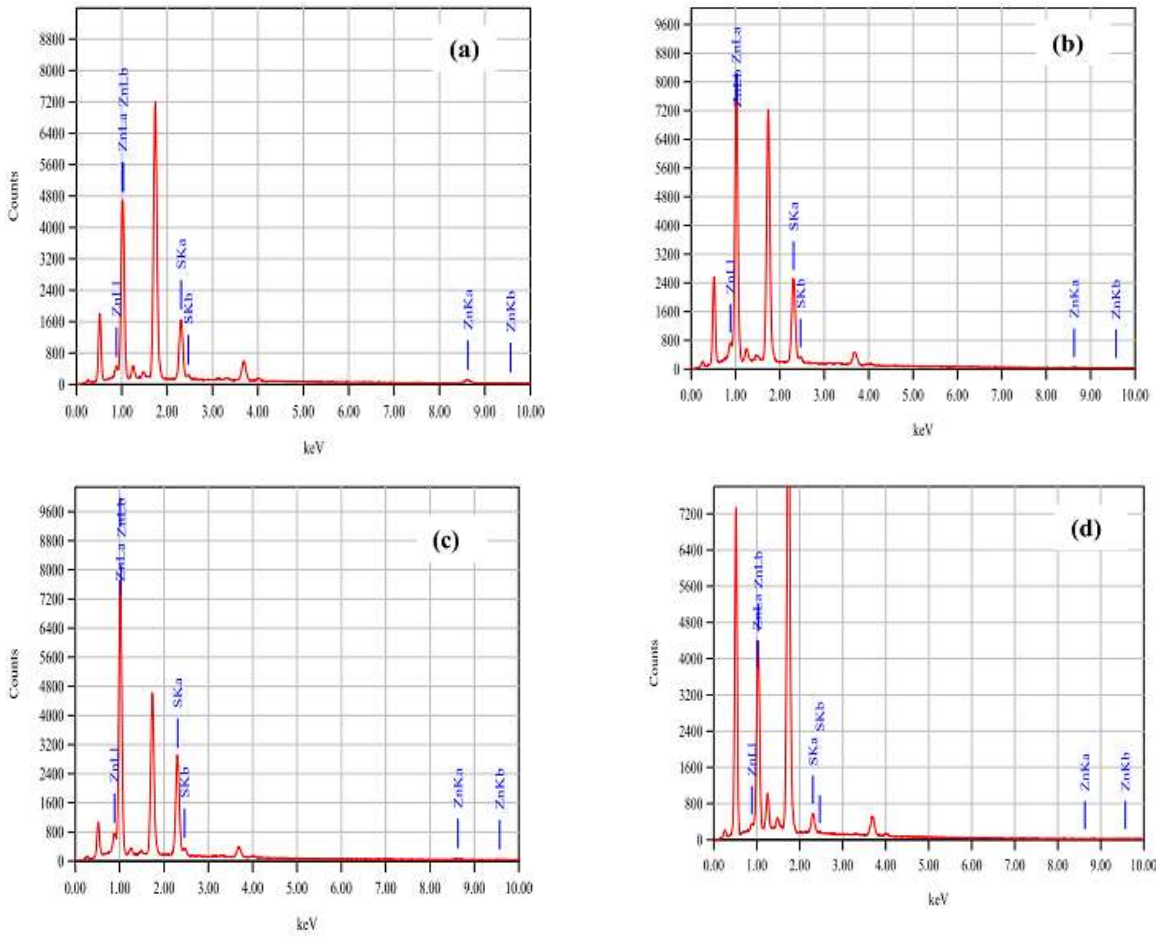

Fig.1 EDX spectra of the deposited ZnS films at (a) RT, (b) 100, (c) 150, and 250°C

Table 1 EDS analysis of ZnS thin films deposited at various substrate temperatur

Substrate temperature (°C)	at.%		Atomic ratio (Zn/S)
	Zn	S	
RT	31.74	68.24	0.465
100	31.05	68.95	0.450
150	38.55	61.45	0.627
250	31.91	68.09	0.468

3.2 Effect of substrate temperature on film thickness

Fig.2 illustrates the relationship between the thickness of the synthesized ZnS films and the substrate temperature. As shown in this figure, it is clearly apparent that the variation in the thickness of the films with temperature can be divided into two regions. In the first region, as the temperature of the substrate increases from room temperature to 150°C , the thickness of the ZnS thin films increases.

The increase in thickness can be described in terms of nucleation. That is, the mobility of incoming atoms on the hot surface is higher, leading to an increase in the nucleation and the film thickness. In the second region, the film thickness gradually decreases above 150°C which can be attributed to re-evaporation of atoms from the film surface. This behaviour is in accordance with the study of Subbaiah et al. **[12].**

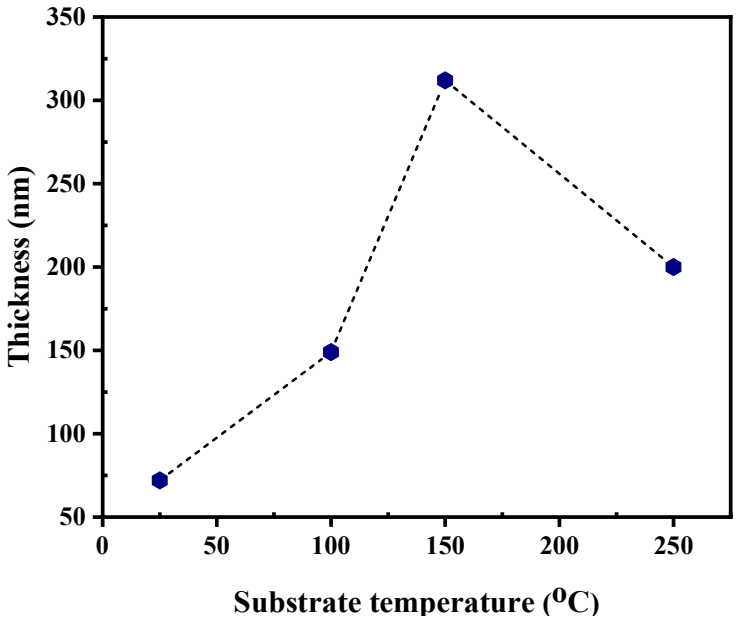

Fig.2 Thickness variation with substrate temperature

3.3 Effect of substrate temperature on structural properties

The XRD patterns of ZnS thin films deposited at various substrate temperatures are shown in **Fig.3**. These patterns reveal that all of the synthetized films are polycrystalline and composed of single sharp (111) diffraction peak, indicating that the grown of the ZnS thin films occur at the preferred orientation of this plane. The diffraction peak corresponded to the cubic structure of ZnS (JCPDF card No. 65-5476). Further, as the substrate temperature increases, the peak intensity increases which owing to the improvement in crystallization. Similar findings have been reported in ZnS thin films prepared on different substrate temperatures via pulsed laser deposition **[6]** and RF magnetron sputtering **[13]**.

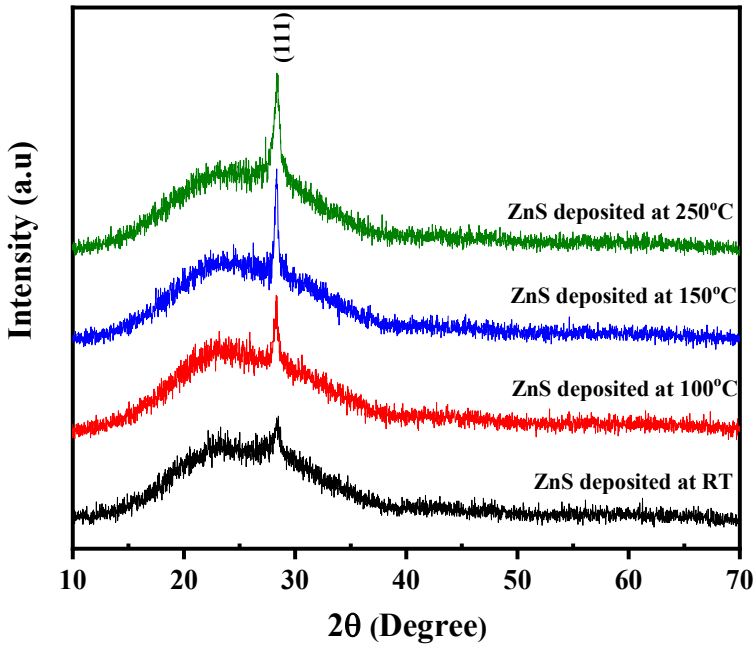

Fig.3 XRD patterns of ZnS thin films at different substrate temperatures.

The lattice constant (a), crystallite size (D), microstrain (ε), and dislocation density (δ) of the prepared films were estimated using the following equations **[5, 14]:**

$$a = \frac{\lambda\sqrt{h^2+k^2+l^2}}{2\,sin\,\theta} \quad \textbf{(1)}$$

$$D = \frac{0.94\,\lambda}{\beta\,\cos\theta} \quad \textbf{(2)}$$

$$\varepsilon = \frac{\beta\cos\theta}{4} \quad \textbf{(3)}$$

$$\delta = \frac{1}{D^2} \quad \textbf{(4)}$$

where h, k and l are the miller indices of the related plane, θ is the Bragger angle, λ is the wavelength of the incident X-ray, and β is the full width half maximum (FWHM). The calculated values are listed in **Table 2**. According to this table, slight change in the lattice parameter values of the deposited ZnS thin films from the standard value 5.41 Å This shift can be explained by the presence of residual stresses wich either due to lattice mismatch or the difference between the thermal expansion coefficients of substrate and film material **[15].** On the other hand, the estimated crystallite size of the growth films is inversely proportional to film thickness which is consistent with previous reports [**11, 16]**. This observed behavior is due to the fact that when the thickness of the film is very low; the interaction between vapour atoms and the substrate will be strong, limiting the mobility of both the ad-atom and the subcritical nuclei. However, as the film thickness rises, the impinging atoms face the

previously formed layer of ZnS. As results, the interaction between substrate and subsequent impinging atoms diminishes as the thickness increases, leading to an enhancement of crystallinity **[16].**

The calculated micro-strain and dislocation density along (111) crystallographic plane for various deposition temperatures are summarized in **Table 2**. The minimum value of the micro-strain and dislocation density is observed for the film deposited at 150°C which indicates a diminution in the lattice imperfections that improve in crystalinity **[5, 17].**

Table 2 Estimated values of the structural parameters of thermally evaporated ZnS thin films deposited at different substrate temperatures.

Substrate temperature (°C)	2θ (°)	a(Å)	D (nm)	$\varepsilon \times 10^{-2}$	$\delta \times 10^{15}$ (Line/m^2)
RT	28.440	5.429	14.316	2.362	4.848
100	28.310	5.453	18.151	1.944	3.035
150	28.310	5.453	25.049	1.444	1.593
250	28.340	5.407	17.859	2.026	3.135

3.4 Effect of substrate temperature on morphological properties

The surface morphology of the deposited ZnS thin films was examined through AFM. The typical 2D and 3D micrographs with the measured area of 5×5 μm^2 are illustrated in **Fig.4**. As shown, AFM micrographs displayed an entire glass substrate coated with spherical form grains and characterize by a strong adhesion without any cracks. However, some pin-holes appeared on the film surface deposited at 100°C. In addition, root mean square (RMS) was evaluated for the thermally evaporated ZnS thin films deposited at different substrate temperatures and regrouped in **Table 2**. According to this table, the obtained values range from 2.12 to 3.61nm, which are significantly lower than those reported by Yang et al. **[6]** on ZnS films grown by pulsed laser deposition. Therefore, this kind of smoother films can be used in solar cell applications, where smooth and regular morphology surface is required for optimal device performance **[18].** Moreover, the grain size of the deposited films is evaluated by using J-Image and is found to gradually increase from about 90 to 250 nm as the substrate temperature increases up to 150°C (**Table 2**). Nevertheless, there is no further increase in grain size as the temperature rises to 250°C.

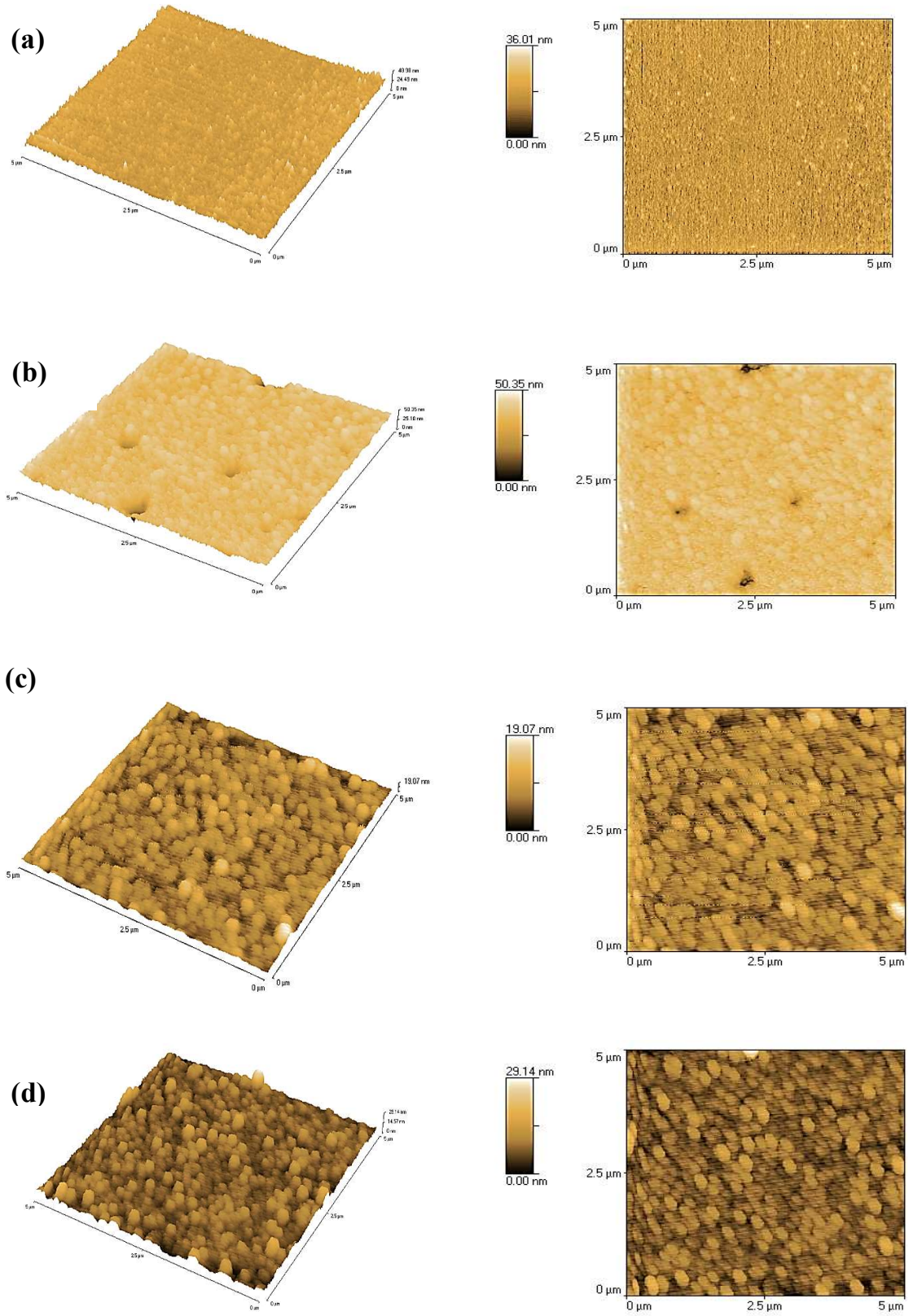

Fig.4 AFM images of ZnS films deposited on glass substrate at (a) RT, (b) 100°C, (c) 150°C and (d) 250°C

Table 3 Grain size, root mean square (RMS), and optical band gap of thermally evaporated ZnS thin films deposited at different substrate temperatures

Substrate temperature (℃)	Average grain size (nm)	RMS (nm)	E_g (eV)
RT	90	3.24	3.52
100	155	3.61	3.71
150	250	2.12	3.40
250	250	2.45	3.80

3.5 Effect of substrate temperature on optical properties

3.5.1 Transmittance and absorbance spectra

Fig. 5 a and **b** illustrate the transmittance and absorbance spectra of the grown ZnS thin films at different deposition temperatures over the wavelength range of 200–800 nm. The transmittance spectra show that all the films are opaque to UV light but transparent to visible light **(Fig. 5 a)**. However, the lower transparency in the visible light was recorded in ZnS film deposited at RT, whereas increasing the substrate temperature led to an increase in transparency up to ~87% for the deposited film at 250**°**C**.** Thus, the increase in substrate temperature can enhance the potential of the thin films in transmitting visible light**.** In general, the film transmittance increases with the reduction in film thickness. Nonetheless, in our study, the transmittance improvement could not be explained in terms of film thickness, because as the substrate temperature increased, the films became thicker **(Fig.2).** Enhancement in the optical transmittance reported for ZnS films may lead to an increase in crystalline quality and a decrease in crystalline defects **[9, 20].** This high transparency suggests that the fabricated ZnS films may use as an alternative buffer layer of CdS in CIGS based solar cells. Moreover, the absorption edges are sharp, confirming the good homogeneity of the synthesized films **[21];** and they exhibit a blue shift when the substrate temperature rises, which could be due to grain size and degree of crystallinity **[6].** Besides, the absorption spectra (**Fig. 5b)** revealed that all the synthesized films exhibit high absorption in the UV light region and very low absorption in the visible region which is consistent with the band gap energy of the ZnS structure. Furthermore, it can also be seen that the film grown at 250°C exhibits a high absorption of UV light in the vicinity of 94%.

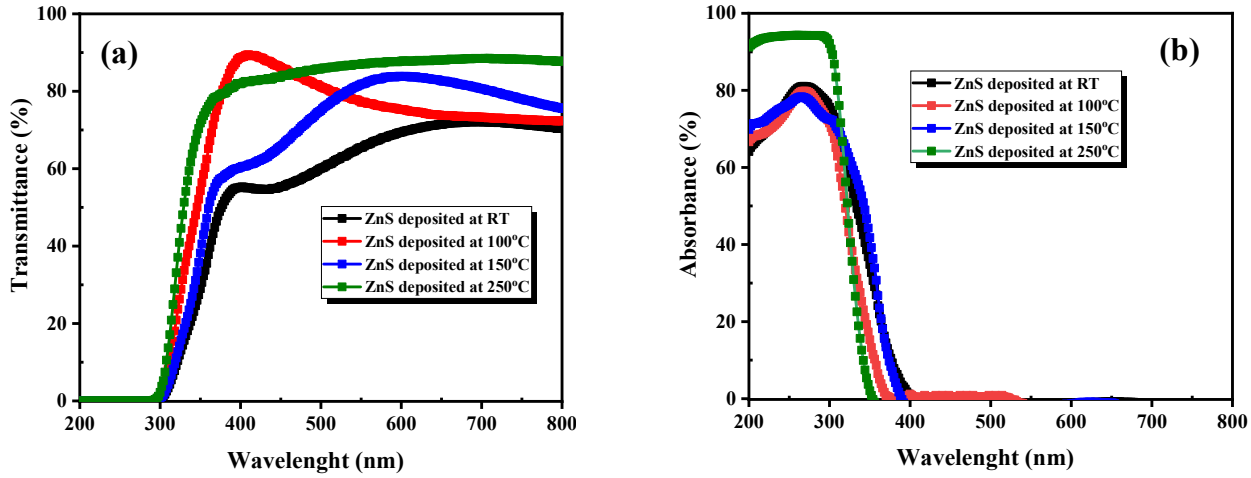

Fig.5 Optical (a) transmittance and (b) reflectance spectra of ZnS thin films grown at different substrate temperatures

3.5.2 Optical band gap energy

The optical direct band gap energy Eg, of the prepared films is estimated with the help of absorption spectra using the following the as-well known Tauc's equation:

$$(\alpha h\nu) = k(h\nu - E_g)^m \quad \textbf{(5)}$$

where hυ denotes incident photon energy, k proportionality constant, m denotes the nature of the electronic, and α is absorption coefficient calculated as follows:

$$\alpha = \frac{2.303}{t} A \quad \textbf{(6)}$$

where t is the film thickness and A its absorbance.

The semiconductor exhibits a direct band gap when m = 1/2, but an indirect band gap when m = 2. $(\alpha h\nu)^2$ versus hν are plotted and depicted in **Fig.6**. The energy gap values of grown films are obtained by extrapolating the sharp linear portion of plots $(\alpha h\nu)^2 = 0$ and listed in **Table 3**. According to this table, the band gap energy increases first from 3.52 to 3.71eV for the synthesized ZnS films grown at RT and 100°C, respectively. Indeed, the band energy is strongly related to the l microstructure of the films, which is principally affected by deposition technique as well as experimental parameters. Yang, et al. **[6]** reported that the substrate temperature caused an enlargement of band gap energy (3.38-3.63 eV) of ZnS thin films prepared by pulsed laser deposition. Zakerian and Kafashan **[22]** reported an increase in the band gap energy of ZnS thin films prepared through an electrochemical route after annealing. Winding in band gap energy is accompanied with an increase in crystallite size which is caused by crystalline quality **[22]** and Burnstein-Moss effect **[23, 24].** After that, the band gap energy shows an opposite behavior regarding the crystallite size.

This finding is in line with the studies of Wu et al. (3.74 to 3.50 eV) **[25]**, Derbali et al. (3.92 to 3.56 eV) **[23],** Ghezali et al. (3.74 to 3.50 eV) **[5],** and Vishwakarma (3.49 to 3.43 eV) **[26].** This behavior can be explained by the quantum size effect **[27].** The film grown at 250°C exhibits a higher band gap energy (3.80 eV) which can be used as a window layer in solar cell.

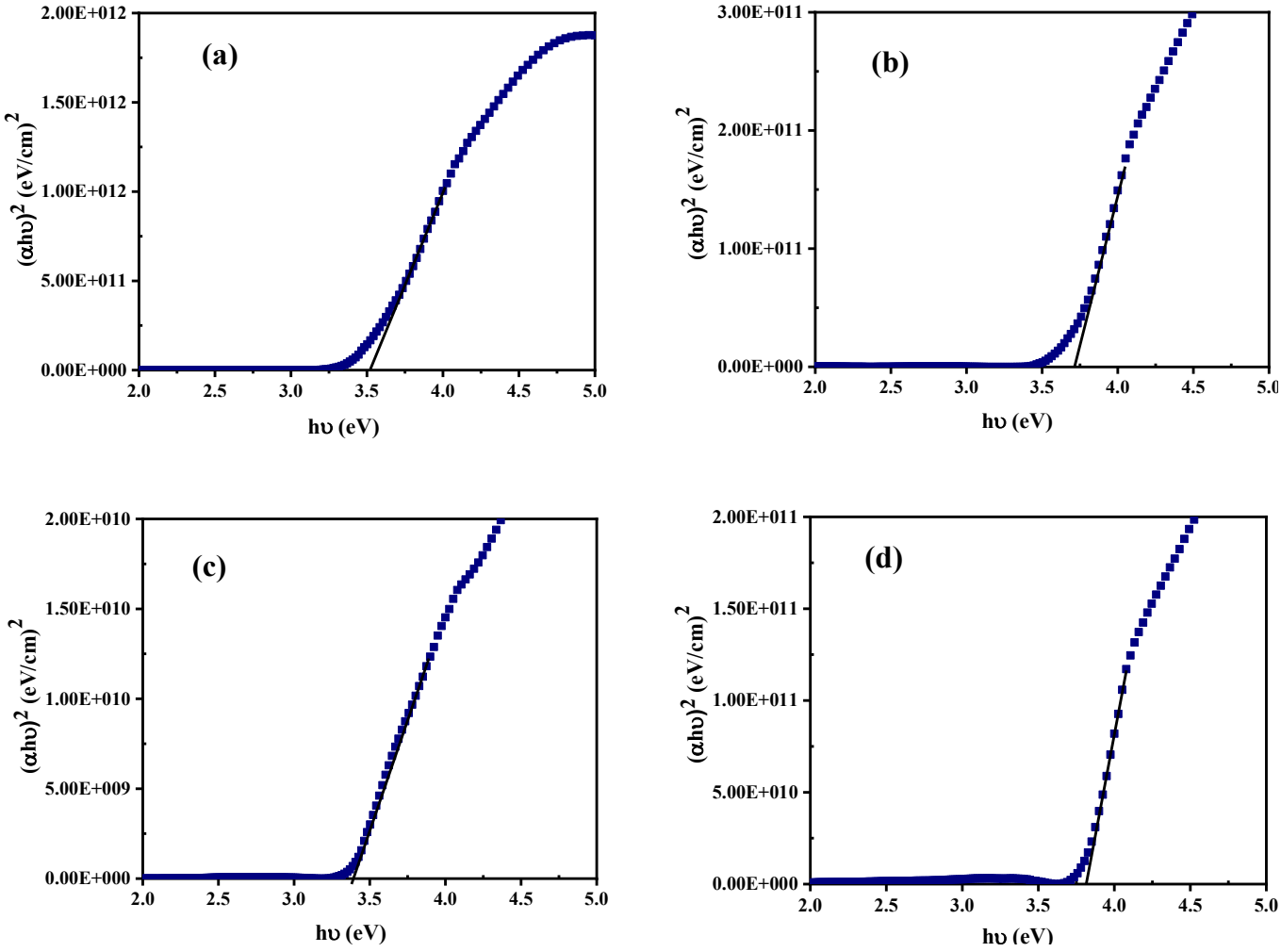

Fig.6 Plots of $(\alpha h\nu)^2$ vs. hν profiles of ZnS films grown on glass substrate at (a) RT, (b) 100°C, (c) 150°C, and (d) 250°C

3.5.3 Refractive index

Estimation of the refractive indices of the prepared films is essiantial for the applications in integrated optics devices. In this study, refraction index of the thermaly avaporated films on various substrate temperature are determinated using the following models **[27, 28]**:

Herve–Vandamme model:

$$n = \sqrt{1 + \left(\frac{13.6}{E_g + 3.47}\right)^2} \quad \textbf{(7)}$$

Reddy model:

$$n = \left(\frac{154}{E_g - 0.365}\right)^{\frac{1}{4}} \quad \textbf{(8)}$$

Kumar and Singh model:

$$n = 3.3668\ (E_g)^{-0.3224} \quad \textbf{(9)}$$

It can be noted in the above models that the refractive index is inversely proportional to the band gap energy. **Table 4** shows the band gap energy reliability ranges based on these models **[27, 28].** In this study, the calculated band gap energies of the deposited ZnS films were between 3.52 and 3.81eV, indicating that the refractive index values based on these models were valid.

Fig. 7 illustrates the plot of the refractive index against substrate temperature for the three models. One can conclude that all the models possess the same pattern between the energy band gap and refractive index. However, Herve–Vandamme and Kumar and Singh models gave almost the same refractive values. The computed refractive indices of ZnS thin films fabricated using the ultrasonic spray technique at various deposition times using the Herve-Vandamme model is reported in eairly study **[23]**. The obtained values were found to be ranging from 2.11 to 2.21, which are simalar to the values calculated in our study (2.121-2.217).

The refractive index of the elaborated films at 150°C exhhibited the maximum value (**Fig. 7**). In fact, the refractive index could be influenced by the microstructure, such as packing density and crystalline quality, and the surface morphology of a prepared film. In our study, the maximum value recorded in the films deposited at 150°C may be attributed to the increase in the crystallinity degree, which is confirmed by XRD analysis.

Table 4 Reliability of band gaps ranges based on the models **[27, 28]**

Model	Reliability Ranges of E_g
Herve-Vandamme	2.00 eV < E_g < 4.00 eV
Reddy	1.10 eV < E_g < 6.20 eV
Kumar and Singh	2.00 eV < E_g < 4.00 eV

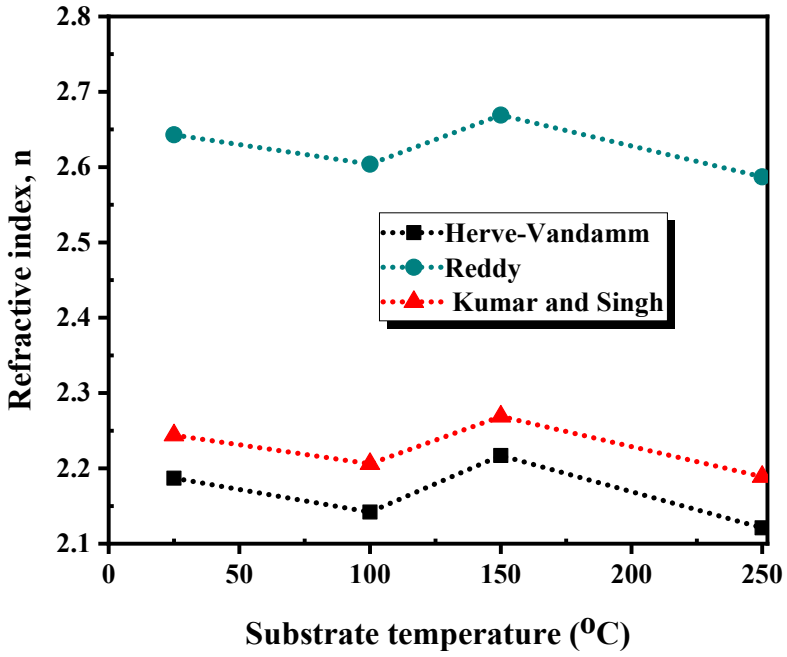

Fig.7 Refractive index against substrate temperature of thermally deposited ZnS films using three different models

4. Conclusion

High purity ZnS thin films have been successfully prepared on glass substrates via thermal evaporation at different substrate temperatures. XRD analysis revealed that the synthesized films were grown along the (111) cubic zinc blend structure direction and their crystallinity improved as the substrate temperature increases. AFM micrographs showed an enhancement of surface roughness of the ZnS films and an increase in grain size from ~90 to 450 nm with increasing substrate temperature. The film deposited at 250°C exhibited high transparency in the visible light and broaden bang gap (~3.80 eV). Furthermore, the estimated refractive index of the deposited ZnS films using Herve–Vandamme and Kumar and Singh models are found to be from 2.121 to 2.217.

Acknowledgments

Fatima G. Al-Badrany would like to thank the Department of Physics, College of Science, Taibah University, for providing support for the implementation of this work in the laboratories of the Physics Department and for facilitating the necessary measurements.

References

[1] Benamra, H., Saidi, H., Attaf, A., Aida, M. S., Derbali, A., & Attaf, N. (2020). Physical properties of Al-doped ZnS thin films prepared by ultrasonic spray technique. *Surfaces and Interfaces*, *21*, 100645.

[2] Martínez-Martínez, S., Mayén-Hernández, S. A., de Moure-Flores, F., Arenas-Arrocena, M. C., Campos-González, E., Zamora-Antuñano, M. A., ... & Santos-Cruz, J. (2016). Sulfiding effects on ZnS thin films obtained by evaporation technique. *Vacuum*, *130*, 154-158.

[3] Hennayaka, H. M. M. N., & Lee, H. S. (2013). Structural and optical properties of ZnS thin film grown by pulsed electrodeposition. *Thin Solid Films*, *548*, 86-90.

[4] Goudarzi, A., Langroodi, S. M., Arefkhani, M., & Langeroodi, N. S. (2022). Study of optical properties of ZnS and MnZnS (ZnS/MnS) nanostructure thin films; Prepared by microwave-assisted chemical bath deposition method. *Materials Chemistry and Physics*, *275*, 125103.

[5] Ghezali, K., Mentar, L., Boudine, B., & Azizi, A. (2017). Electrochemical deposition of ZnS thin films and their structural, morphological and optical properties. *Journal of Electroanalytical Chemistry*, *794*, 212-220.

[6] Yang, K., Li, B., & Zeng, G. (2019). Effects of temperature on properties of ZnS thin films deposited by pulsed laser deposition. *Superlattices and Microstructures*, *130*, 409-415.

[7] Özkan, M., Ekem, N., Pat, S. U. A. T., & Balbağ, M. Z. (2012). ZnS thin film deposition on Silicon and glass substrates by Thermionic vacuum Arc. *Materials science in semiconductor processing*, *15*(2), 113-119.

[8] Kunapalli, C. K., Chakraborty, D., & Shaik, K. (2021). Effect of vacuum annealing on structural, optical and magnetic properties of Sn doped ZnS thin films. *Optical Materials*, *114*, 110961.

[9] Guzeldir, B., Saglam, M., & Ates, A. (2012). Deposition and characterization of CdS, CuS and ZnS thin films deposited by SILAR method. *Acta Physica Polonica-Series A General Physics*, *121*(1), 33.

[10] Wu, X., Lai, F., Lin, L., Lv, J., Zhuang, B., Yan, Q., & Huang, Z. (2008). Optical inhomogeneity of ZnS films deposited by thermal evaporation. *Applied Surface Science*, *254*(20), 6455-6460.

[11] Priya, K., Ashith, V. K., Rao, G. K., & Sanjeev, G. (2017). A comparative study of structural, optical and electrical properties of ZnS thin films obtained by thermal evaporation and SILAR techniques. *Ceramics International*, *43*(13), 10487-10493.

[12] Subbaiah, Y. V., Prathap, P., & Reddy, K. R. (2006). Structural, electrical and optical properties of ZnS films deposited by close-spaced evaporation. *Applied Surface Science*, *253*(5), 2409-2415.

[13] Hwang, D. H., Ahn, J. H., Hui, K. N., San Hui, K., & Son, Y. G. (2012). Structural and optical properties of ZnS thin films deposited by RF magnetron sputtering. *Nanoscale research letters*, *7*(1), 1-7.

[14] Akyuz, I., & Yeni, I. (2021). Effect of Heat Treatment in Different Atmospheres on Thermally Evaporated ZnS films. *Optical Materials*, *119*, 111381.

[15] Ohring, M. (2001). *Materials science of thin films*. Elsevier.

[16] Prathap, P., Revathi, N., Subbaiah, Y. V., & Reddy, K. R. (2007). Thickness effect on the microstructure, morphology and optoelectronic properties of ZnS films. *Journal of Physics: Condensed Matter*, *20*(3), 035205.

[17] Purohit, A., Chander, S., Sharma, A., Nehra, S. P., & Dhaka, M. S. (2015). Impact of low temperature annealing on structural, optical, electrical and morphological properties of ZnO thin films grown by RF sputtering for photovoltaic applications. *Optical Materials*, *49*, 51-58.

[18] Keshav, R., & Mahesha, M. G. (2018). Photoluminescence and Raman spectroscopic analysis of PV deposited ZnS thin films. *Materials Research Bulletin*, *105*, 360-367.

[19] Fathy, N., & Ichimura, M. (2005). Photoelectrical properties of ZnS thin films deposited from aqueous solution using pulsed electrochemical deposition. *Solar Energy Materials and Solar Cells*, *87*(1-4), 747-756.

[20] Daranfed, W., Aida, M. S., Hafdallah, A., & Lekiket, H. (2009). Substrate temperature influence on ZnS thin films prepared by ultrasonic spray. *Thin Solid Films*, *518*(4), 1082-1084.

[21] Agrawal, D., Suthar, D., Agarwal, R., Patel, S. L., & Dhaka, M. S. (2020). Achieving desired quality of ZnS buffer layer by optimization using air annealing for solar cell applications. *Physics Letters A*, *384*(24), 126557.

[22] Zakerian, F., & Kafashan, H. (2018). Investigation the effect of annealing parameters on the physical properties of electrodeposited ZnS thin films. *Superlattices and Microstructures*, *124*, 92-106.

[23] Derbali, A., Attaf, A., Saidi, H., Benamra, H., Nouadji, M., Aida, M. S., ... & Ezzaouia, H. (2018). Investigation of structural, optical and electrical properties of ZnS thin films prepared by ultrasonic spray technique for photovoltaic applications. *Optik*, *154*, 286-293.

[24] Joishy, S., Hebbar, D. N., Kulkarni, S. D., Rao, K. G., & Rajendra, B. V. (2020). Band structure controlled solid solution of spray deposited Cd1-x ZnxS films: Investigation on

photoluminescence and photo response properties. *Physica B: Condensed Matter*, *586*, 412143.

[25] Wu, X., Lai, F., Lin, L., Lv, J., Zhuang, B., Yan, Q., & Huang, Z. (2008). Optical inhomogeneity of ZnS films deposited by thermal evaporation. *Applied Surface Science*, *254*(20), 6455-6460.

[26] Vishwakarma, R. (2015). Effect of substrate temperature on ZnS films prepared by thermal evaporation technique. *Journal of Theoretical and Applied Physics*, *9*(3), 185-192.

[27] Tripathy, S. K. (2015). Refractive indices of semiconductors from energy gaps. *Optical materials*, *46*, 240-246.

[28] Senol, S. D., Ozugurlu, E., & Arda, L. (2020). Synthesis, structure and optical properties of (Mn/Cu) co-doped ZnO nanoparticles. *Journal of Alloys and Compounds*, *822*, 153514.